Gate Leakage vs. NBTI in Plasma Nitrided Oxides: Characterization, Physical Principles, and Optimization

*[1]A.E. Islam, [2]G. Gupta, [2]S. Mahapatra, [3]A.T. Krishnan, [4]K. Ahmed, [4]F. Nouri, [5]A. Oates, [1]M.A. Alam

*Email: aeislam@purdue.edu, Phone: 765-494-5988, Fax: 765-494-6441

[1]Electrical and Computer Engineering, Purdue University, West Lafayette, IN, USA; [2]Department of EE, IIT Bombay, India; [3]Texas Instruments, Dallas, TX, USA; [4]Applied Materials, Inc., Santa Clara, CA, USA; [5]Taiwan Semiconductor Manufacturing Corp., Hsin-Chu, Taiwan.

Abstract

Since nitrided oxides improve gate leakage at the expense of NBTI, one must optimize nitrogen concentration in oxinitride samples for reliable performance and reduced power dissipation. Here, we analyze wide range of NBTI stress data to develop a predictive model for gate leakage and first self-consistent model for field acceleration within R-D framework. This model anticipates a novel design diagram for co-optimization of leakage and NBTI for arbitrary nitrogen concentration and effective oxide thickness.

1. Introduction

Since nitrided oxides (SiON) improve gate leakage (J_G) [1-6] at the expense of NBTI performance (ΔV_T) [7,8], one must necessarily optimize N_2 concentration (%N) in gate-oxides for high-performance ICs. Despite its importance, however, a quantitative analysis of leakage/NBTI trade-off (as a function of %N), has never been reported and the question "Is co-optimization of NBTI/leakage possible at any %N?" has never been answered. In this paper, we simultaneously measure gate leakage and delay-free NBTI over broad range of stress-fields, stress-temperatures and %N, model gate leakage current (J_G) and NBTI degradation within a theoretically consistent framework (hole-assisted thermal generation of interface traps) of field-dependent R-D model, and conclude that although there is no optimum %N for NBTI/leakage, the reduction in J_G at NBTI-limited %N (~15-25%, depending on failure criterion) can be significant and would reduce power dissipation without affecting NBTI-margin.

2. Gate Leakage

Comprehensive simulation [9] (which includes the effects of multi-subband electron/hole quantization, poly-depletion, *etc.*) of the measured J_G-V_G for both N- and PMOS (Fig. 1) was done to extract the model parameters as a function of %N (Fig. 2). We assume that any variation in the spatial-profile of nitrogen results only in second-order correction to calculated J_G. Contrary to popular belief [2-6, 10], the oxide parameters do not scale linearly with %N. All the parameters have approximately a quadratic fit with %N. Here, effective oxide thickness *(EOT)* is obtained from simulation of CV, and physical thickness (T_{PHY}) and %N are determined by XPS [11]. These %N-dependent parameters are used to calculate $J_G(N,EOT)$ for arbitrary %N and *EOT*, as shown in Fig. 10b.

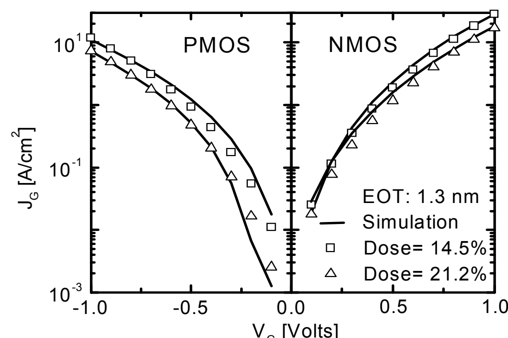

Fig. 1: Experimental leakage current (J_G) vs. gate voltage (V_G) curves for SiON devices (14.5% and 21.2% N_2 dose) in inversion region, fitted using simulation.

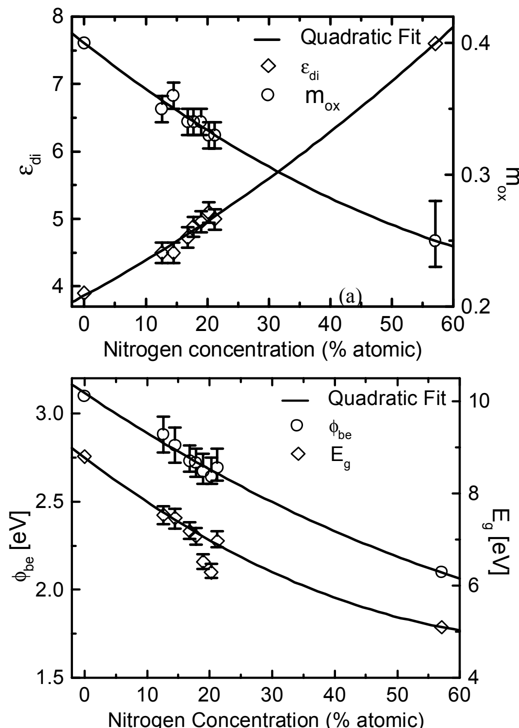

Fig. 2: Variation of gate leakage model parameters with %N (0% for SiO_2, 57.1% for Si_3N_4) (a) relative permittivity for SiON dielectric, ε_{di} and oxide effective mass, m_{ox} (b) barrier height for electron, φ_{be} and bandgap, E_g. For Si_3N_4, parameters are obtained from references [2-6] (φ_{be}: 2.1 eV, E_g: 5.1 eV, ε_{di}: 7.6, m_{ox}: 0.23~0.28). The error bars show the variation in parameters expected due to ±0.5 Å error in measurement of T_{PHY} by XPS.

1-4244-0439-8/06/$20.00 ©2006 IEEE

3. Reliability based on NBTI

NBTI performance for different SiON devices is monitored here by calculating safe operating voltage *(V_{safe})*, which is defined as the stress voltage at which device can operate up to its lifetime *(t_{life})* without crossing the failure criteria (e.g. 60mV of ΔV_T [1]). As shown in Fig. 3, degradation data taken at different stress voltages *(V_1, V_2, V_3, V_4)* can be fitted with analytical expressions, based on the field-dependent R-D model to be discussed Section 3.1. Such fitting can be used to extract lifetimes *(t_1, t_2, t_3, t_4)* at stress voltages and V_{safe}, based on failure criteria. The calculated $V_{safe}(N,EOT)$ for arbitrary %N and *EOT* is plotted in Fig. 10a.

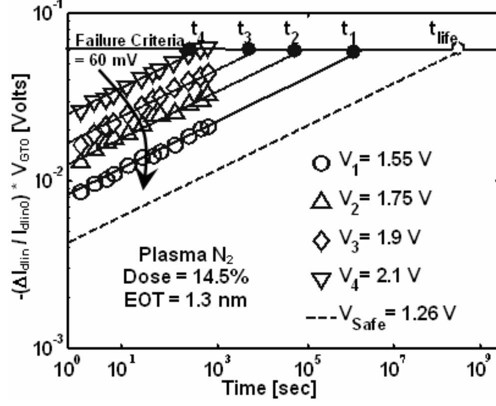

Fig. 3: Procedure for obtaining lifetimes *(t_1, t_2, t_3, t_4)* at different stress voltages *(V_1, V_2, V_3, V_4)* and V_{Safe} using NBTI model, discussed in section 3.1. Proper V_G-E_{ox} transformation is used here and I_{dlin0} was obtained within 1ms of application of stress.

3.1 Field-Dependent R-D model

Since NBTI is field-dependent [12], the E_{ox} (calculated either from direct integration of CV, or approximated using proper V_G-E_{ox} relationship) dependence of NBTI parameters needs to be established. The R-D model anticipates that [13]

$$\Delta N_{IT} \sim (k_{f0}N_0/k_{r0})^{2/3}\{D_0 exp(-E_D/k_BT)t\}^{1/6} \quad (1)$$

for neutral-H_2 diffusion [13-15], which is supported by delay-free NBTI measurements [13-16]. Since the diffusion co-efficient pre-factor, $D_0=l^2v_0$ (l is lattice constant, v_0 is attempt frequency) is field-independent, NBTI field-dependence must be encapsulated in the ratio of forward (k_{f0}) and reverse (k_{r0}) dissociation constants, i.e. k_{f0}/k_{r0}. Such model assumes that holes [$p_h \propto E_c$; the field due to mobile carriers] at the Si/SiON interface tunnel into [probability, $P_T \sim exp(\gamma_T E_{ox})$] and is captured by Si-H bonds [cross-section, σ] ~2Å away from the interface, leading to a hole-assisted, field-enhanced, thermal generation [rate, $B \propto exp(-(E_{F0}-aE_{ox})/k_BT)$] of interface traps (Fig. 4). Based on these relations, Eqn. (1) transforms to

$$\Delta N_{IT} = A|Ec|^{2/3} exp(2\gamma E_{ox}/3) exp(-nE_{D1}/k_BT)t^n \quad (2)$$

where, $\gamma=\gamma_T+a/k_BT$, $nE_{D1}= nE_D+2/3(E_{F0}-E_{R0})$; $n\sim 1/6$.

Eq. (2) suggests the overall activation energy for ΔN_{IT} will be

$$E_{IT} = nE_A = nE_D + 2/3(E_{F0} - E_{R0} - aE_{ox}). \quad (3)$$

The assertion that NBTI degradation is field-driven is well known [12, 13] and easily established by Fig. 5 and R-D analysis of wide variety of stress data (Fig. 6). The explicit parameterization of this E_{ox} dependence is discussed below.

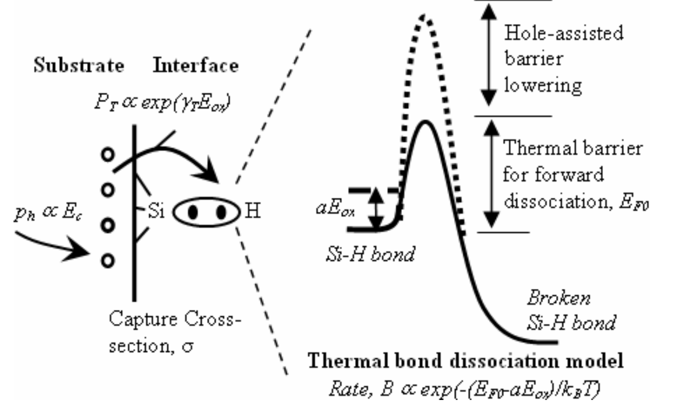

Fig. 4: Hole-assisted, field-enhanced model for Si-H thermal bond dissociation. k_{r0} is assumed to field independent to first order.

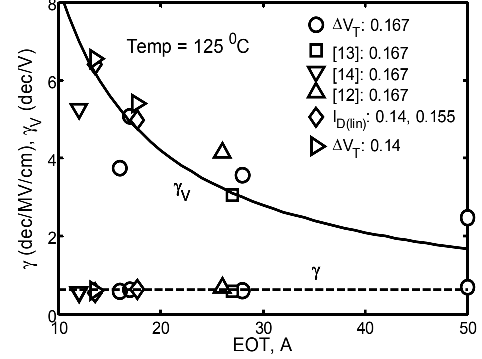

Fig. 5: γ and γ_V (voltage acceleration factor) [12] variation with *EOT* (*n* is mentioned for each case). For field-dependent NBTI model, γ remains almost constant (~0.6±0.05; dashed line) and $\gamma_V \sim 1/EOT$ (solid line) [12]. For ΔV_T measurements, necessary delay correction is done.

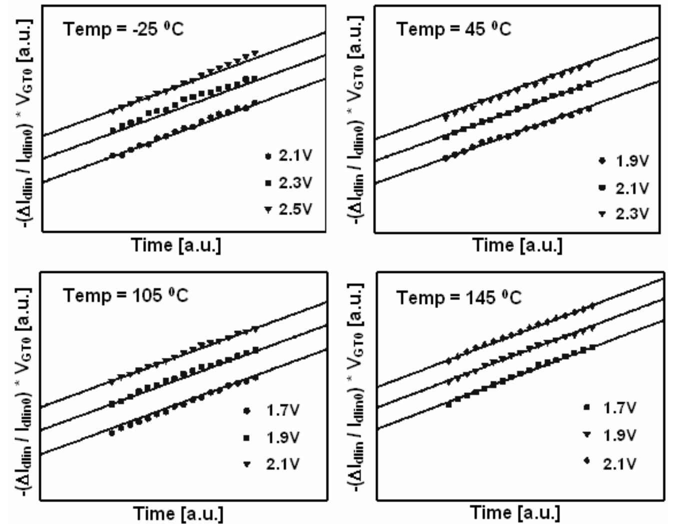

Fig. 6: Fitting ΔV_T vs. t (log-log scale) at different T and V_G by (2), validates the universality of the model, which gives A, γ, n as fitting parameters for each temperature (effect of E_{D1} can be included in A). Here n =0.15~0.16, indicating H_2 diffusion and N_2 dose: 8%

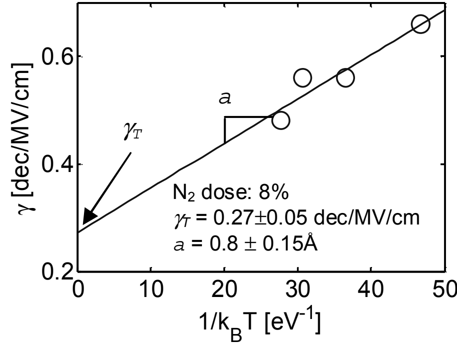

Fig. 7a: γ vs. $1/k_BT$ plotting. γ obtained from Fig. 6 is used here. The obtained γ_T = 0.27±0.05 dec/MV/cm and a = 0.8 ± 0.15Å

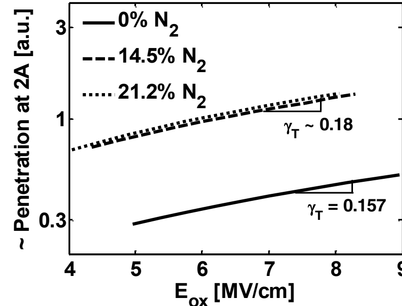

Fig. 7b: Wavefunction penetration at 2 Å (from C-V analysis) modeled using $A_1 exp(\gamma_T E_{ox})$. Analytically [19], $\gamma_T \sim \sqrt{(m_{ox}/\varphi_{bh})}$ and $A_1 \sim exp\sqrt{(m_{ox}\varphi_{bh})}$, which are consistent with the obtained variations using parameters of Fig. 2.

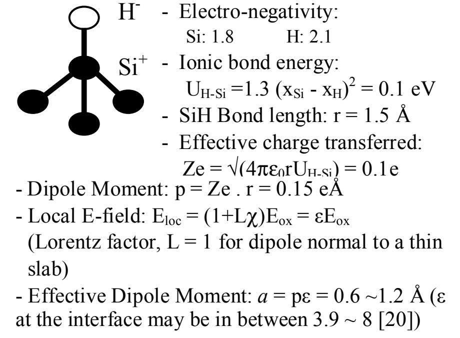

Fig. 7c: Polarization properties of SiH bond, indicating a = 0.6 ~ 1.2 Å. [21]

3.2 Extraction of γ_T and a

The tunneling coefficient γ_T can either be determined by the *intercept* of measured γ (extracted from Fig. 6) vs. $1/k_BT$ plot (Fig. 7a) or estimated by the simulation of $P_T(E_{ox})$ (Fig. 7b, based on parameters from Fig. 2). Both approaches provide comparable results. Similarly effective dipole moment a can either be measured from *slope* of γ vs. $1/k_BT$ plot (Fig. 7a) and/or from E_A vs. E_{ox} variations (Fig. 9), or be theoretically estimated by molecular modeling approach (Fig. 7c). The summary in Table 1 shows that theory and measurements provide remarkably consistent results. Therefore, part of the E_{ox}-dependencies of NBTI arises from E_{ox}-dependence of P_T and the other part, from E_{ox}-induced thermal barrier lowering, B (Fig. 9). This, we believe, is the first consistent interpretation of field-dependence of NBTI degradation within the R-D framework. Previous analysis of delay-contaminated NBTI data [17] suggested experimental values of a that was 3~4 times larger than theoretically expected values. It appears that similar to resolution of puzzles involving time-exponent (n=0.25→0.16) and temperature dispersion parameter (d=0.6→0) [13], zero-delay measurements and partitioning γ_T into $\gamma_T + a/k_BT$ (previous work incorrectly assigns $\gamma = a/k_BT$ [17] or $\gamma = \gamma_T$ [12] exclusively) hold the key for consistent estimation of field-acceleration of NBTI degradation.

3.3 Parametric dependence on %N

The methodologies discussed above have been used to analyze the E_{ox} and T-dependent NBTI data at various %N to determine $\gamma(N)$ [= $\gamma_T(N) + a(N)/k_BT$] and $E_A(N)$ (see Fig. 8, 9). While γ_T depends weakly on %N (Fig. 7b), $a(N) = k_BT\,[\gamma(N) - \gamma_T(N)] \sim 0.25\, dE_A/dE_{ox}$ and $E_A(N)$ shows systematic variation with %N (Fig. 8, 9 [18]). Hence, our analysis shows that the NBTI degradation with %N variation can be attributed to three factors: reduction of over-all barrier height for dissociation nE_{D1}, variation in $A(N)$ and modification of effective dipole moment a, with negligible contributions from induced hole density (p_h).

4. Optimization

The parameters of $\gamma(N)$, $E_A(N)$, $a(N)$, $n(N)$, derived by fitting the NBTI data and encapsulated within the field-dependent R-D model discussed above, can now be used to calculate $V_{safe}(N,EOT)$ for any combinations of %N and EOT (Fig. 10a). Fig. 11 summarizes the results for $J_G(N,EOT)$ and $V_{safe}(N,EOT)$, indicating that co-optimization for DC-NBTI and ITRS-limited J_G [1] may sometimes require reduced temperature, inclusion of AC effects [23], and NBTI aware design [24]. The diagram can be used to calculate any pair of the variables (V_{safe}, J_G, $\%N$, EOT) when the other pair is given. For example, if an IC design requires V_{safe} = 1.1V and

TABLE 1
Comparing a determined by various methodologies

a [Å]	Obtained from		
0.8	Fit of $\gamma = \gamma_T + a/k_BT$	Fig. 7a	Experiment
0.86 (avg.)	$a = (\gamma - \gamma_T)k_BT$	Fig. 8	
0.98 (avg.)	$a = 0.25\, dE_A/dE_{ox}$	Fig. 9	
1.47	$a = (\gamma - \gamma_T)k_BT$ *	[17]	
0.6~1.2	Si-H polarization	Fig. 7c	Calculation
0.65 (avg.)	First Principle†	[22]	

* γ obtained after delay correction and $\gamma_T \sim 0.27$. In reference, a = 3.2 Å
† For Equilibrium structure

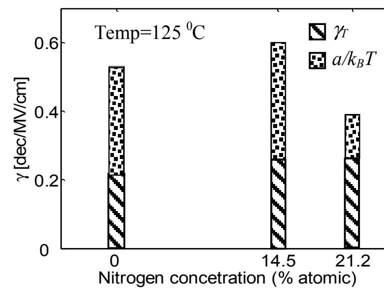

Fig. 8: Variation of γ with %N, after fitting degradation curves for SiON devices, using (2). As stated in the text, γ will have two parts γ_T ~ 0.225, 0.27, 0.27 (from Fig. 7a and 7b) and a/k_BT.

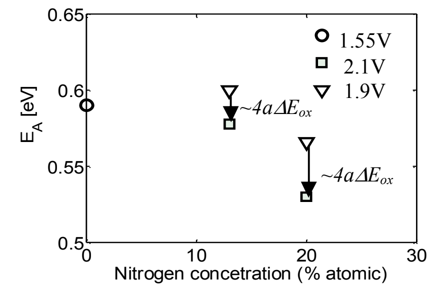

Fig. 9: E_A determined for various sample. With change in %N, there is a systematic variation in E_A. There is also slight decrease in E_A with increase in V_G, because $E_A = E_D + 2/3n(E_{F0} - E_{R0} - aE_{ox})$.

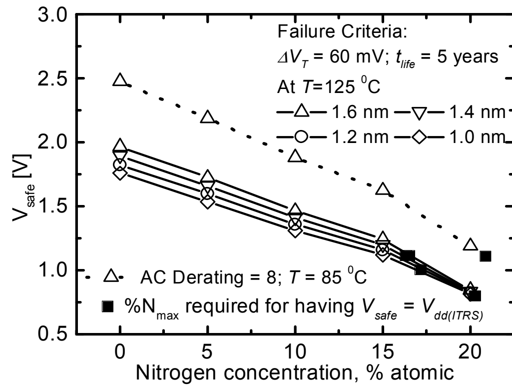

Fig. 10a: V_{safe} vs. %N at different *EOT* (Failure criteria: ΔV_T = 60 mV, t_{life}=5 years[1]). Dotted line for 1.6 nm *EOT* indicates the improvement with AC derating = 8 and T = 85 ^{0}C.

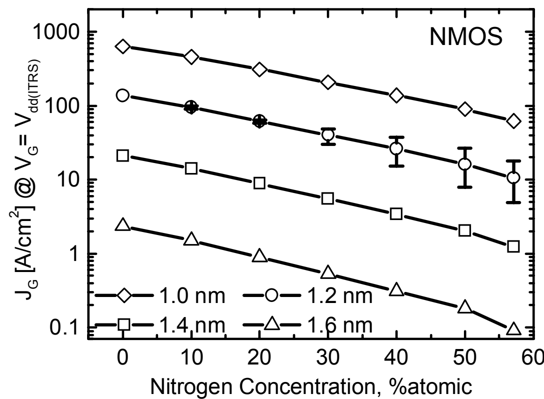

Fig. 10b: J_G @ $V_{dd(ITRS)}$ for NMOS vs. %N for different *EOT*. The error bar @1.2 nm indicates J_G variation, expected due to ±0.5 Å error in T_{PHY}, which is negligible upto 30% N_2 dose.

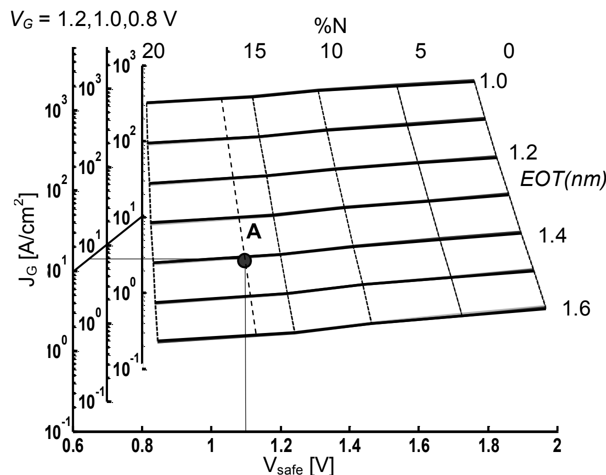

Fig. 11: Design diagram for SiON devices, obtained by using Fig. 10a and 10b (J_G @ V_G = 0.8, 1.0, 1.2V are considered). Example**:** choose V_G= V_{safe} from x-axis and J_G from V_G specific y-axis, then read off corresponding %N and *EOT*. Inclusion of AC effects and temperature reduction will right-shift the diagram, thus enabling co-optimization at smaller *EOT*.

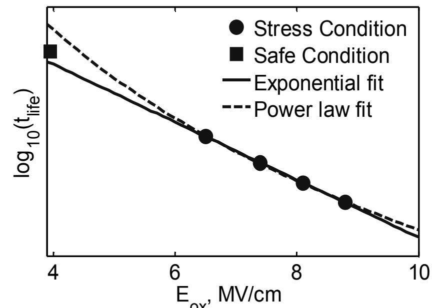

Fig. 12: Comparison between exponential and power law fit of ΔV_T data for obtaining safe operating condition using stress data. Procedure in Fig. 3 used for obtaining safe condition. Exponential fit underestimates and power law fit overestimates t_{life}.

J_G = 10A/cm^2 (point A, Fig. 11), the design diagram suggests an *EOT* = 1.4nm and %N ≅ 17%.

5. Conclusion

We have analyzed an extensive set of NBTI data to develop the first self-consistent model for field acceleration within R-D framework (compared with other empirical formulation in Fig. 12), constructed a novel design diagram for co-optimization of J_G and NBTI for arbitrary %N and *EOT* combinations, and established the DC (AC)-NBTI limited upper limit of %N ~ 15-20% (20-25%) for core CMOS technologies. We anticipate that our analysis would have broad impact for optimization of %N content in sub-2nm gate dielectrics.

Acknowledgement

This work was done with financial support from TI, AMAT, TSMC, Renesas and SRC. We also acknowledge NCN for providing computational resources.

References

[1] ITRS 2005 version.
[2] M.L. Green et al., *JAP*, 90(5), p. 2057, 2001.
[3] P.A. Kraus et al., *TED*, 52(6), p. 1141, 2005.
[4] G. Lucovsky et al., *JVST -A*, 18(4), p. 1163, 2000.
[5] X. Guo et al., *EDL*, 19(6), p. 207, 1998.
[6] H.Y. Yu et al., *TED*, 49(7), p. 1158, 2002.
[7] S.S. Tan et al., *APL*, 82(12), p. 1881, 2003.
[8] D.K. Schroder et al., *JAP*, 94(1), p. 1, 2003.
[9] A. Ghetti et al., SISPAD, p. 239, 1999.
[10] D.M. Brown et al., *JES*, 115(3), p. 311, 1968.
[11] J.R. Shallenberger et al., *JVST -A*, 17(4), p. 1086, 1999.
[12] M.A. Alam et al., *Micro. Reliability*, 45(1), p. 71, 2005.
[13] D. Varghese et al., IEDM, p. 684, 2005.
[14] S. Chakravarthi et al., IRPS, p. 273, 2004.
[15] A.T. Krishnan et al., IEDM, p. 688, 2005.
[16] C.L. Chen et al., IRPS, p. 704, 2005.
[17] K.O. Jeppson et al., *JAP*, 48(5), p. 2004, 1977.
[18] J.P. Campbell et al., IRPS, p. 442, 2006.
[19] Register et al., APL, 74(3), p. 457, 1999.
[20] Muller et. al. Nature, 399(6738), 1999.
[21] Mcpherson et. al., JAP, 84(3), p. 1513, 1998.
[22] Ushio et al., JAP, 97(8), 2005.
[23] M.A. Alam, IEDM, p. 345, 2003.
[24] B.C. Paul et al., *EDL*, 26(8), p. 560, 2005.